Int. J. Electrochem. Sci., 13 **(2018)** 10679 – 10687, doi: 10.20964/2018.11.26

International Journal of ELECTROCHEMICAL SCIENCE
www.electrochemsci.org

Short Communication

Confined Preparation of N-doped Commercial P25 TiO_2 Photocatalysts with Fast Charge Separation by Argon-diluted Nitrogen Plasma Treatment

Shifei Kang[1], *Lu Zhang*[1], *Tao Xu*[2], *Maofen He*[1], *Mengya Chen*[1], *Qiuhe Wang*[2], *Di Sun*[3,*], *Xijiang Chang*[1,*]

[1] Department of Environmental Science and Engineering, University of Shanghai for Science and Technology, Shanghai, 200093, China.
[2] School of Electrical & Electronic Engineering, Shanghai University of Engineering Science. Shanghai, 201620, China.
[3] Department of Ultrasound in Medicine, Shanghai Jiao Tong University Affiliated Sixth People's Hospital & Shanghai Institute of Ultrasound in Medicine, Shanghai, 200233, China.
[*]E-mail: sundy316@163.com, 091031001@fudan.edu.cn

Received: 27 June 2018 / *Accepted:* 20 August 2018 / *Published:* 1 October 2018

N-doped TiO_2 attracts enormous attention due to its cheapness and excellent visible-light-driven photocatalytic activity. An approach assisted by Nitrogen plasma to synthesize the N-doped TiO_2 is presented in our work by using commercial available Degussa P25 as raw material. X-ray photoelectron spectroscope (XPS) and transmission electron microscope (TEM) measurement results show that the evidence of N doping and the formation of surface disorder layer, which can both serve as active sites. Electrochemical characterizations verified the excellent photo-generated charge separation feature of the obtained N-doped P25 TiO_2. High absorption of visible light, fast charge separation and numerous active sites ensure the excellent photocatalytic activity for the N-doped P25 TiO_2 in the photo-oxidation of organic molecules in water. It is noteworthy that the Argon-assistant Nitrogen plasma treatment is superior to conventional pure Nitrogen plasma treatment because of confined Nitrogen ionization. From the results, this plasma treatment method may open up a new way to the application of plasma technology in the activation commercial materials.

Keywords: N-doped TiO_2, Plasma Treatment, Charge Separation, Transient photocurrents

1. INTRODUCTION

Titanium dioxide (TiO_2) is very promising for environmental applications, such as photocatalytic hydrogen generation and pollutant removal, owing to its strong optical absorption,

chemical stability, low cost and high reactivity. However, the large electronic bandgap of 3.0–3.2 eV restricts its optical absorption mainly to the ultraviolet (UV) region, which accounts for only 4% of natural solar energy.[1] More seriously, the serious recombination of photoinduced charges restricted the quantum efficiency of TiO_2.[2, 3] For these reason, many studies have been conducted to improve the visible light absorption and photogenerated charges separation of TiO_2 over years, for example, the incorporation of light-absorbing materials (sensitizer, quantum dots, dyes) and the modification of TiO_2 electronic properties by adding dopants (transition metals, nitrogen, sulfur, phosphorus).[4, 5] However, transition metal centers in TiO_2 may act in some cases as electron-hole recombination centers, thus reducing the overall photocatalytic activity. More recently, researchers have paid much attention in the use of non-metals dopants and particularly nitrogen.

Reports indicate N/TiO_2 exhibits modified optical properties upon the onset of visible light absorption and is catalytically active in various reactions under visible light irradiation.[6] A number of methods are available for the preparation of N-doped TiO_2 photocatalytic, including sol–gel (Dong et al., 2015;Yoko et al., 1987)[7,8], electrochemical (Brezesinski et al., 2009)[9],hydrothermal (Liu et al., 2016)[10], sputtering (Amor et al., 1997)[11],and chemical deposition (Puma et al., 2008)[12] methods. Unfortunately, most of the reported methods are energy-consuming and expensive, or even involve environmentally unfriendly reagents. Meanwhile, the identification of the active nitrogen center responsible for photoactivity is seldom discussed based on electrochemical observations in the system, which plays an effective role in photoactivity.

Herein, we report a simple, fast and mass-producible approach assisted by discharge plasma treatment to produce N-doped TiO_2 photocatalysts. We tried to use the confined microwave surface-wave plasma technology to ionize Argon and Nitrogen mixture gas in a vacuum chamber for surface modification of TiO_2 powder. This plasma-treated TiO_2 nanostructure showed strong visible light absorption. We elucidated the inner workings of this TiO_2 nanostructure are that excellent electrochemical performance was yielded to broaden the visible light absorption region and provide numerous active sites for photo-degradation.

2. EXPERIMENTAL SECTION

2.1. Materials preparation

Commercial Degussa P25 TiO_2 composed of 80% anatase and 20% rutile was purchased from Evonik Degussa company and was used as raw materials in the powered form. The plasma source was a self-designed microwave plasma generator as shown in Scheme 1. Better than traditional thermal plasma processing by dielectric barrier discharge(DBD) plasma or capacitive coupled plasma mode, the self-designed microwave plasma generator are much better in the processing efficiency and scale, which can active materials in gram level within 5 minutes, or treat materials in kilogram level with magnified equipment.[13] The plasma treated P25 TiO_2 power was developed by uniformly covering with 1 g of TiO_2 power on the sample table in the centre of the reaction chamber. The gas control system and pumping system worked together to adjust the working gas composition and pressure. A 1kW microwave source (MUEGGE, MS1000B)was employed and plasma can be excited in the

processing chamber under a suitable gas condition after energy coupling and in the surface-wave mode. We focused on the effect of N_2 plasma treatment on the samples for 5 min. Before plasma ignition, the processing chamber was pumped to a basis vacuum of about 10-2 Pa and then was filled with nitrogen (99.999%). The chamber can be sustained by a mass flow controller at pressure of about 20 Pa. When the microwave was turned on and the sub-tuner was tuned, plasma can be excited in the chamber. The argon-diluted nitrogen plasma used in some references consisted of more effective particles or functional group compared to pure nitrogen plasma. Thus, we used two plasma mode by using different gas, that is pure N_2 and a mixture gas of N_2:Ar with a mole ratio 1:3.[13-15] The sample obtained by are named as TiO_2-N_2 and TiO_2-N_2+Ar, respectively.

2.2. Characterization

The Bruker Advanced D8 powder X-ray diffractometer (XRD, Germany) was operated under Cu-Kα radiation (λ = 1.5418 Å) at a scan step of 0.02°. The Thermo ESCALAB 250 X-ray photoelectron spectroscope (XPS) was run under Al Kα monochromatization. The JEM-2100F transmission electron microscope (TEM) was operated at an accelerating voltage of 200 kV. Brunauer-Emmett-Teller (BET) specific surface area (S_{BET}) was measured with a Micromeritics Tristar 3000 analyzer at 77.4 K and pore size distribution was determined by the Barrett-Joyner-Halenda (BJH) method. The Cary 500 ultraviolet-visible (UV-vis) diffuse reflectance spectrophotometer (DRS) was run with BaSO4 as the reference. Electrochemical impedance spectroscopy (EIS) and transient photocurrents were recorded by a Chi660e electrochemical workstation based on a conventional three-electrode system from frequency 0.01 Hz to 100 kHz at the circuit potential.

2.3. Photocatalytic activity measurement

Photocatalytic oxidation activity of each sample was preliminarily investigated by monitoring the degradation of a Rhodamine B (Rh B) aqueous suspension (20 mg/L, 50 mL) in a quartz tube added with 50 mg of a catalyst. Visible light irradiation was supplied by a 500 W Xe lamp light source with a 420 nm optical filter, and light intensity on the quartz tube was 20 mW/cm2. The Rh B concentration was analyzed by recording the absorbance of its characteristic peak at 554 nm using an Evolution Thermo 600 UV-vis spectrophotometer.

3. RESULTS AND DISCUSSION

3.1. Characteristicsof catalysts

TEM images (Fig.1) of the prepared TiO_2-N_2+Ar show that the obtained treated TiO_2 nanoparticles are about 20 nm in diameter and have a nitrogen-stabilized amorphous layer surrounding a crystalline core to form an amorphous shell/crystalline core structure. The lattice spacing in TiO_2-N_2+Ar was determined to be 0.35 nm, corresponding to the (101) plane of the anatase poly-crystal phase, which is similar with former reports on the P25 TiO_2 nanoparticles.[13] The disordered surface

layer about 0.5 nm thick is coated on a crystalline core after the Ar-assisted nitrogen plasma process, which is not exist in the untreated P25 nanoparticles. These observations indicate that the crystal structure remains stable after plasma treatment, while the surface features changed, which may in favor of the separation of photo-generated charges.[16]

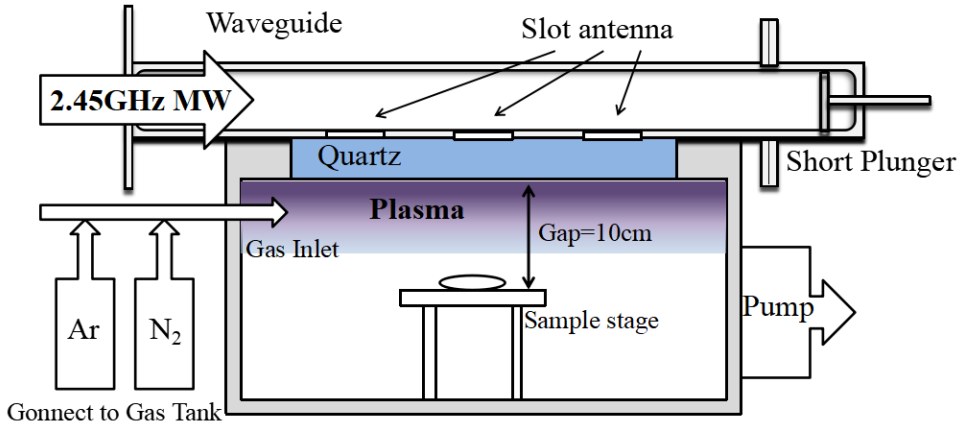

Scheme 1. The Simulation diagram of the self-designed microwave plasma generator.

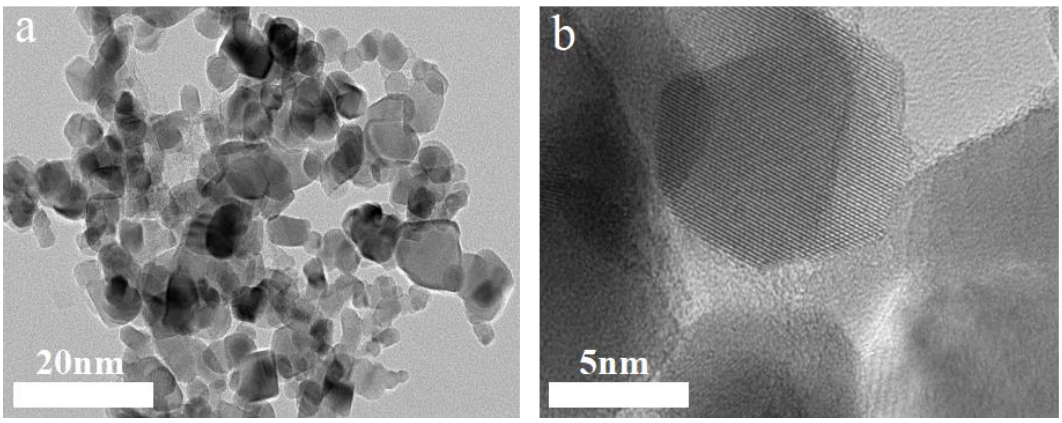

Figure 1. TEM images of black TiO_2–N_2+Ar

The crystallinity degrees of N-doped TiO_2-N_2, and TiO_2-N_2+Ar after each plasma treatment, as well as the original P25 TiO_2, were verified by XRD (Fig. 2a). The peaks at 2θ = 25.3, 37.8, 48.0, 53.9, 55.1, 62.7, 68.9 and 70.3 °are indexed to anatase TiO_2, while the planes at 2θ = ca. 27.4, 36.1 and 41.2° are ascribed to rutile TiO_2.[17] All samples show a mixture of anatase and rutile phases similar with the standard mode of commercial P25 TiO_2. The intensity of the main peak (1 0 1) of anatase or (1 1 0) of rutile was not significantly changed after the plasma treatment, indicating the high-intensity plasma treatment has a negligible effect on the phase transition of TiO_2 polymorphs. The structural stability was further examined by measuring Raman scattering, and six Raman active modes (3Eg + 2B1g + A1g) were found at frequency 144, 197, 399, 515, 519 (superimposed with the 515 cm−1 band), and 639 cm−1, respectively.[5]

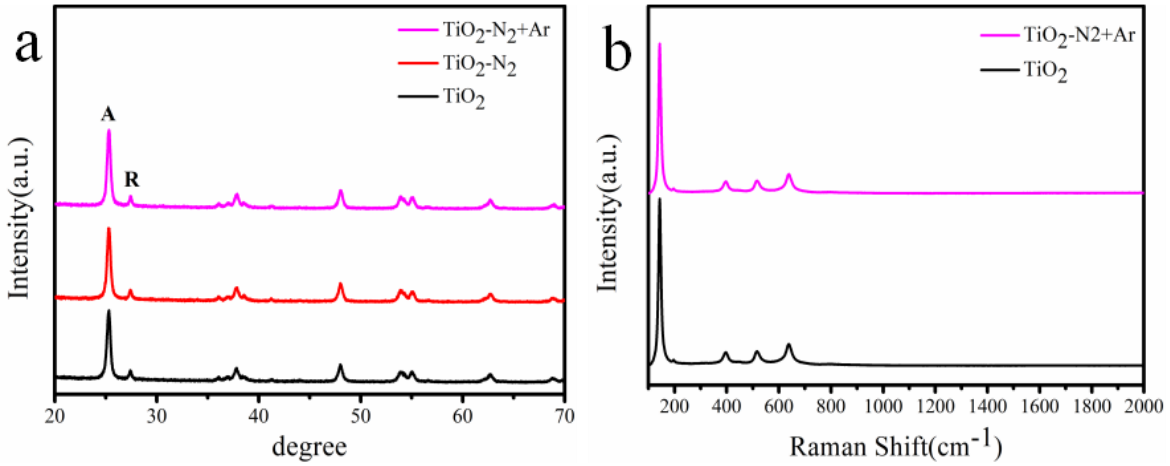

Figure 2. (a) XRD patterns after different N_2 plasma treatments (A = anatase, R = rutile); (b) Raman spectra of the samples

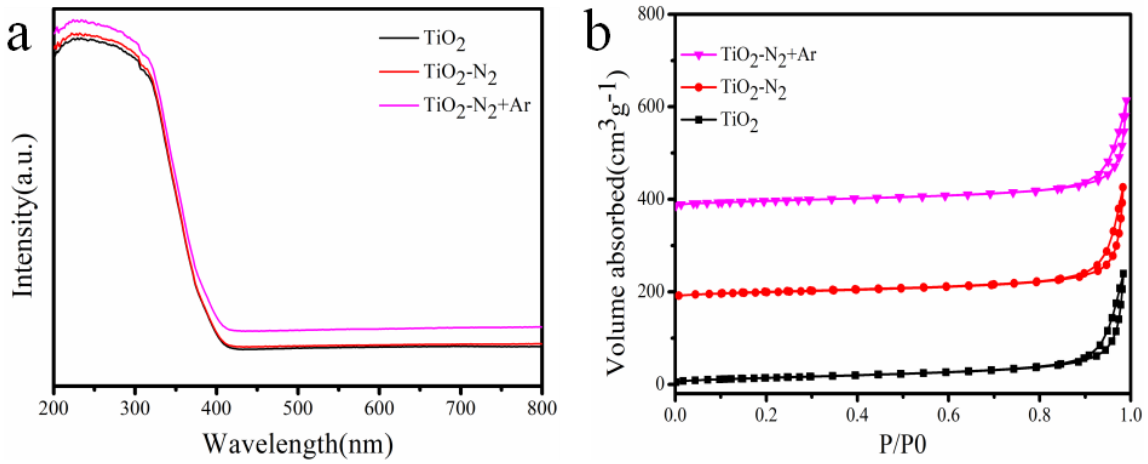

Figure 3. (a) UV-vis spectra of the samples; (b) Nitrogen adsorption–desorption isotherms.

Table 1. BET specific surface areas and nitrogen contents of TiO_2 and TiO_2-N_2+Ar

	TiO_2	TiO_2-N_2+Ar
S_{BET} (m^2/g)	27.07	56.35
N content (wt.%)	1.02	2.28

Figure 3a shows the UV-vis spectra of the samples. Clearly, strong absorption over bare P25 TiO_2, TiO_2-N_2 and TiO_2-N_2+Ar was found in the UV region, but not in the visible region (> 420nm) except for the TiO_2-N_2+Ar sample. The BET surface areas of commercial P25 TiO_2 and TiO_2-N_2+Ar were 27.07 and 56.35 m^2/g, respectively (Table 1). These results are consistent with our expectation that the presence of numerous nanopores in TiO_2 during N_2/Ar electrical discharge treatment resulted in a nanoporous structure. In other words, the discharge plasma treatment affect the BET surface area

and pore size distribution that correlate with photocatalytic activity.[18] Moreover, the majority of TiO_2-N_2+Ar nanopores showed broad peaks at 20 nm, which correspond to a typical IV isotherm with a H3-type hysteresis loop mainly located at 0.85 < P/P0 < 0.98 (Fig. 3b).

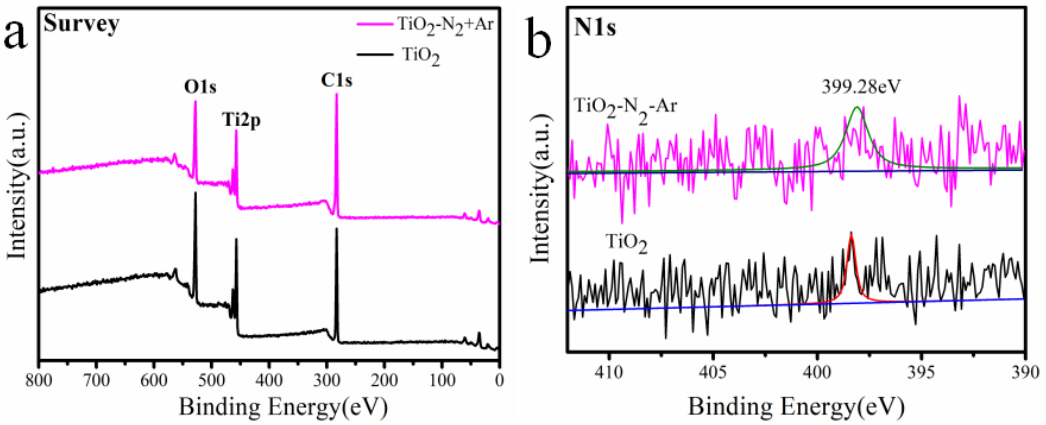

Figure 4. (a) Ti2p XPS spectra and (b) N1s spectra of samples

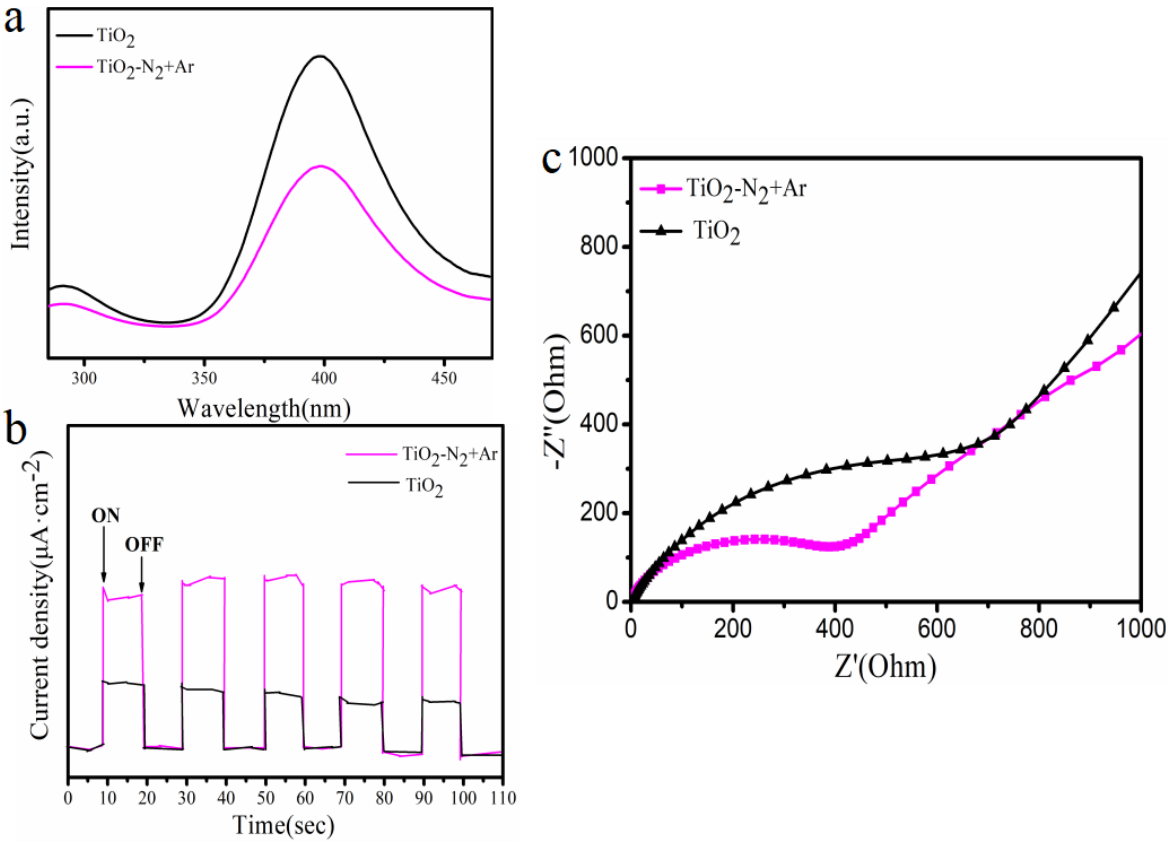

Figure 5. (a) PL spectra and (b) Transient photocurrents under visible light irradiation; (c) EIS spectra of different samples.

The effect of Ar-assisted nitrogen plasma on the chemical bonding state of TiO_2 was investigated via XPS. The C 1s, O 1s and Ti 2p were observed from all the samples (Fig. 4a). The N 1s XPS spectra of TiO_2 and TiO_2-N_2+Ar display only one N 1s core level peak at ca. 399.28 eV, indicating the two samples contain uniform N species.[19] In addition, the atomic concentration of N 1s of TiO_2-N_2+Ar was 2-fold higher than that of TiO_2 (Table 1). The optimum N concentration indicates the Ar-assisted nitrogen plasma can improve the N doping in TiO_2.[20]

The effective transfer of photogenerated charge carriers depends sensitively on the trap sites in the semiconductor, which are closely related to the structural defects of the material. Clearly, both samples show a strong intrinsic PL peak at ~400 nm, though the intensity is much lower over TiO_2-N_2+Ar (Fig. 5a), which indicates the weakened recombination of photo-generated electron-hole pairs, and thus favors an enhanced photocatalytic performance.[21] As the considerable change in band gap could enhance photoelectrochemical activity, we measured the photocurrent of the samples under the irradiation of a Xe lamp. When the UV light source was turned on, the photocurrent density of the proton beam-irradiated TiO_2-N_2+Ar was 2.2 times that of the bare TiO_2 (Fig. 5b). The larger photocurrent could be also attributed to the higher electron–hole separation efficiency under light irradiation.[22] Also, the proton beam irradiation for nitrogen doping could be used to improve the photoelectrochemical activity of the P25 TiO_2. The EIS Nyquist plots of P25 TiO_2 and the TiO_2-N_2+Ar electrodes under visible light irradiation are shown in Fig. 5c. The arc radius on EIS Nyquist plot of TiO_2-N_2+Ar is much smaller than P25 TiO_2. As reported, a smaller arc radius of the EIS Nyquist plot suggests a more effective separation of photogenerated electron-hole pairs and the faster interfacial charge transfer.[23, 24] These results suggest the TiO_2-N_2+Ar sample has dramatically smaller charge transfer resistance and higher electron-hole separation/transfer efficiency. The enhanced photoelectric properties can be attributed to the surface disorder layer that greatly facilitates the mass transfer and improves photogenerated charge mobility.

3.2. Photocatalytic activity

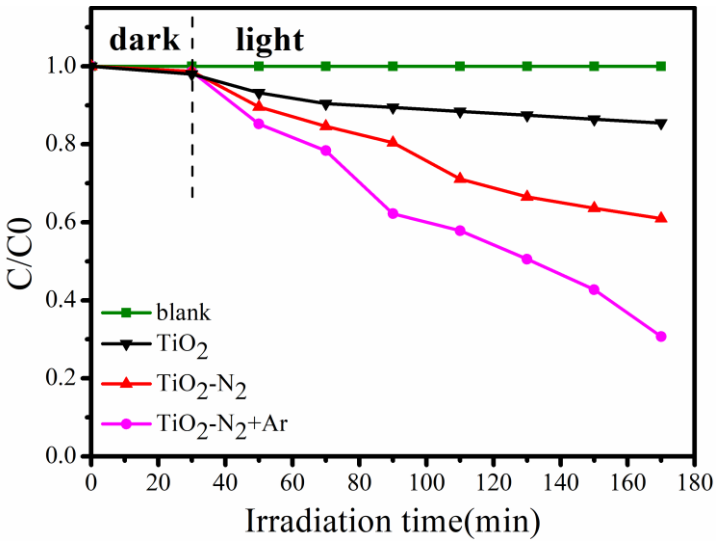

Figure 6. Photocatalytic curves on Rh B degradation over different photocatalysts under visible light irradiation.

As showed in Fig. 6, except for the slight adsorption in dark time, the photocatalytic efficiency of pure TiO2 after 140 min of irradiation is only 10%. With the N_2 plasma treatment, the Rh B photodegradation was comparatively increased. Remarkably, because of assisted-Ar in the N_2 discharge plasma treatment can efficiently dope more active sites of N on the surface of TiO_2, TiO_2-N_2+Ar was efficient in photocatalytic degradation and removed nearly 70% of Rh B within 140 mins.[24, 25] In consideration of the ability of rapid and low cost material activation of plasma treatment, this technology is promising in industrial applications in pursuit of high-quality catalysts.[26]

4. CONCLUSIONS

A simple, low-cost and environmental-friendly plasma treatment method was developed and used to prepare scalable and clean nanoporous TiO_2 photocatalysts with larger surface area and higher electron transport ability. The TiO_2-N_2+Ar shows much superior photocatalytic activity in water purification. The photoactivity of the treated samples, especially the TiO_2-N_2+Ar sample, was much higher than that of plain TiO_2. The significantly improved photoactivity of TiO_2-N_2+Ar sample can be ascribed to the enlarged specific surface area, bordered visible light absorption and fast charge separation, which was introduced by the confined Argon-diluted Nitrogen plasma treatment to produce amorphous surface layer and more active sites. This work provides insights for the industrial application of plasma technology in materials modification.

ACKNOWLEDGEMENTS
This work was financed by the National Natural Science Foundation of China (Grant No. 11705115, 51502172 and 81701697), Med-X Project (No: YG2017QN22) supported by Shanghai Jiao Tong University, Program for Professor of Special Appointment (Young Eastern Scholar) at Shanghai Institutions of Higher Learning(No. QD2016036) and Shanghai Local University Young Teacher Training Project (No. ZZGCD16006)

References

1. H.-R. An, S.Y. Park, J.Y. Huh, H. Kim, Y.-C. Lee, Y.B. Lee, Y.C. Hong, H.U. Lee, *Appl. Catal. B: Environ.,* 211 (2017) 126-136.
2. Z. Zhang, X. Wang, J. Long, Q. Gu, Z. Ding, X. Fu, *J. Catal., 276* (2010) 201-214.
3. L. Hu, J. Wang, J. Zhang, Q. Zhang, Z. Liu, *RSC. Adv.,* 4 (2014) 420-427.
4. F. Teng, M. Li, C. Gao, G. Zhang, P. Zhang, Y. Wang, L. Chen, E. Xie, *Appl. Catal. B: Environ.,*148 (2014) 339-343.
5. R. Trejo-Tzab, J.J. Alvarado-Gil, P. Quintana, P. Bartolo-Pérez,*Catal. Today.,* 193 (2012) 179-185.
6. S. Mohajeri, *Int. J. Electrochem. Sc.,* 12 (2017) 5121-5141.
7. R. Dong, F. Wang, Z.Li , Z.Chen, H. Zhang, C. Jin, *Surf. Coat. Technol.,* 276 (2015) 391–398.
8. T. Yoko, K. Kamiya, S. Sakka, *Yogyo.Kyokai.Shi.,* 95 (1987)
9. T. Brezesinski, J. Wang, J. Polleux, B. Dunn, S.H. Tolbert, *J. Am. Chem. Soc.,* 131 (2009) 1802–1809.

10. C. Liu, L.Q. Zhang, R. Liu, Z.F. Gao, X.P. Yang, Z.Q. Tu,F. Yang, Z.Z. Ye, L.S. Cui, C.M. Xu, Y.F. Li, *J. Alloy. Compd.,* 656 (2016) 24-32
11. S.B. Amor, G. Baud, J. Besse, M. Jacquet, *Mater. Sci. Eng.,* B 47 (1997) 110–118
12. G.L. Puma, A. Bono, D. Krishnaiah, J.G. Collin, *J. Hazard. Mater.,* 157 (2008) 209–219.
13. Z. Wang, C. Yang, T. Lin, H. Yin, P. Chen, D. Wan, F. Xu, F. Huang, J. Lin, X. Xie, M. Jiang, *Adv. Funct. Mater.,* 23 (2013) 5444-5450.
14. S. Livraghi, M.C. Paganini, E. Giamello, A. Selloni, C.D. Valentin, G. Pacchioni, *J. Am. Chem. Soc.,* 128 (2006) 15666–15671.
15. R. Asahi, T. Morikawa, T. Ohwaki, K. Aoki, Y. Taga, *Science.,* 293 (2001) 269-271.
16. J. Yang, H. Ding, Z. Zhu, Q. Wang, J. Wang, J. Xu, X. Chang, *Appl. Surf. Sci.,* 454 (2019) 173-180.
17. L.F. Cui, Y.F. Liu, X.Y. Fang, C.C. Yin, S.S. Li, D. Sun, S.F. Kang, *Green. Chem.,* 2018.
18. H. Chen, *Int. J. Electrochem. Sc.,* 13 (2018) 2118-2125.
19. S.F. Kang, L. Zhang, M.F. He, Y.Y. Zheng, L.F. Cui, D. Sun and B. Hu, *Carbon.,* 2018.
20. X. Wang, W. Zhang, L. Wu, F. Ye, J. Xiao, Z. Li, *RSC. Adv.,* 4 (2014) 56567-56570.
21. X. Yang, X. Chang, R. Tei, M. Nagatsu, Journal of Physics D: *Appl. Phys* 49 (2016) 235205.
22. R. Jothi Ramalingam, *Int. J. Electrochem. Sc.,* 12 (2017) 797-811.
23 X.J. She, H. Xu, Y.G. Xu, J. Yan, J.X. Xia, L. Xu, Y.H. Song, Y. Jiang, Q. Zhang, H.M. Li, *J. Mater. Chem.,* A 2 (2014) 2563-2570.
24 H. Xu, J. Yan, X.J. She, L. Xu, J.X. Xia, Y.G. Xu, Y.H. Song, L.Y. Huang, H.M. Li, Nanoscale., 6 (2014) 1406-1415.
25. D. Luo, *Int. J. Electrochem. Sc.,* 13 (2018) 5904-5922.
26. Y.F. Guo, J. Li, Y.P. Yuan, L. Li, M.Y. Zhang, C.Y. Zhou, Z.Q. Lin, *Angew. Chem. Int. Edit.,* 55 (2016) 14693-14697.